

Difference in Narrow Emission Line Spectra of Seyfert 1 and 2 galaxies

Kai Zhang, Tinggui Wang, Xiaobo Dong, Honglin Lu

Center for Astrophysics, University of Science and Technology of China (USTC), Hefei, Anhui, 230026, China; zkdte@mail.ustc.edu.cn, twang@ustc.edu.cn

Joint Institute of Galaxies and Cosmology, USTC and Shanghai Observatory

ABSTRACT

In the unification scheme of Seyfert galaxies, a dusty torus blocks the continuum source and broad line region in Seyfert 2 galaxies. However it is not clear whether or not and to what extent the torus affects the narrow line spectra. In this paper, we show that Seyfert 1 and Seyfert 2 galaxies have different distributions on the $[\text{O III}]/\text{H}\beta$ vs $[\text{N II}]/\text{H}\alpha$ diagram (BPT diagram) for narrow lines. Seyfert 2 galaxies display a clear left boundary on the BPT diagram and only 7.3% of them lie on the left. By contrast, Seyfert 1 galaxies do not show such a cutoff and 33.0% of them stand on the left side of the boundary. Among Seyfert 1 galaxies, the distribution varies with the extinction to broad lines. As the extinction increases, the distribution on BPT diagram moves to larger $[\text{N II}]/\text{H}\alpha$ value. We interpret this as an evidence for the obscuration of inner dense narrow line region by the dusty torus. We also demonstrate that the $[\text{O III}]$ and broad line luminosity correlation depends on the extinction of broad lines in the way that high extinction objects have lower uncorrected $[\text{O III}]$ luminosities, suggesting that $[\text{O III}]$ is partially obscured in these objects. Therefore, using $[\text{O III}]$ as an indicator for the nuclear luminosity will systematically under-estimate the nuclear luminosity of Seyfert 2 galaxies.

Subject headings: galaxies: active–galaxies:Seyfert–(galaxies:) quasars: emission lines

1. Introduction

The unification scheme of Seyfert galaxies has been widely accepted to explain the dichotomy of Seyfert 1 (hereafter Sy1) and Seyfert 2 galaxies (hereafter Sy2) (e.g. Antonucci 1993). The basic idea is that the differences between Sy1s and Sy2s are caused by an

orientation effect. The broad line region (BLR) and continuum source are blocked from our view in Sy2s by thick obscuring material, presumably a dusty torus (Antonucci & Miller 1985) at large inclination angles, while they are observed directly in Sy1s. In both types of Seyfert galaxies, narrow emission lines, produced on a large scale, are observed. This scheme has been supported by many observations (Antonucci & Miller, 1985; Miller & Goodrich, 1990; Klöckner et al, 2003; Greenhill et al, 2003; Jaffe et al, 2004), and even the temperature distribution of the dusty torus has been measured (e.g., Tristram et al, 2007).

While it is general agreed that dusty tori obscure BLR and continuum source, and even the central narrow line region (NLR) of Sy2s (e.g., Rhee & Larkin 2005; Haas et al. 2005), it is still unclear to what extent they obscure the NLR, and how the obscuration depends on the orientation (i.e., the difference in NLR obscuration among different types of Seyfert galaxies). This is an important issue because the narrow line luminosity is often used as a surrogate for the bolometric luminosity of Seyfert 2 nuclei. In addition, it may yield important clues to the structure of NLR. Jackson & Browne (1990) compared [O III] emission from quasars (i.e., radio-loud QSOs) with radio galaxies — both of them are believed to be the analogs of the two types of Seyfert galaxies (Barthel 1989), and found that the [O III] emission of quasars is much stronger than that of radio galaxies. It was interpreted as part of the [O III] emission is obscured by the torus in radio galaxies. A similar conclusion was reached by Haas et al. (2005) by comparing [O III] λ 5007 with [O IV] λ 25.9 μ m. On the other hand, Barthel & Fosbury (1994) showed that, when comparing [O II] emission of quasars and radio galaxies, both classes of objects have very similar distributions, corroborating the obscuration scenario. Unfortunately, [O II] emission may be enhanced by shocks induced by radio plasma (Best et al. 1999) and thus may not be a good tracer of AGN luminosity. Moreover, a fraction of FR II radio galaxies may be intrinsically less luminous than quasars (Ogle, Whysong & Antonucci, 2006; also Meisenheimer et al. 2001).

It is well known that NLR is stratified, at least for AGNs of some sort (e.g., Veilleux et al. 1991, Robinson et al. 1994). Emission lines of higher critical density or ionization potential are produced averagely closer to the active nucleus than those of lower critical density or ionization. This fact can be used to check whether the inner NLR region is blocked by torus in Sy2s; and if yes, to what extended NLR is obscured. Murayama & Taniguchi (1998) found that Sy1s show excess [Fe VII] λ 6087 with respect to Sy2s, and proposed that [Fe VII] arises mainly from the inner wall of dusty tori. Schmitt (1998) compared [O II] λ 3727Å, [Ne III] λ 3869Å, [O III] λ 5007Å, [Ne V] λ 3426Å, as well as 60 μ m continuum flux from a sample of 52 Sy1s to those of 68 Sy2s; they found that Sy1s have higher excitation than Sy2s. However, the differences were interpreted as that Sy1s have smaller number of ionization bounded clouds than Sy2s by him.

In this paper, we study the location of Sy1s and Sy2s on the BPT diagrams, short for Baldwin-Phillips-Terlevich diagrams (Baldwin et al 1981), which are often used for classification of narrow emission line galaxies. With the large spectroscopic sample of both Sy1s and Sy2s available from the Sloan Digital Sky Survey (York et al, 2000), and spectral decomposition, we are able to detect the different distributions of Sy1s and Sy2s on BPT diagrams.

2. Sample and Data Analysis

2.1. Seyfert 1 and 2 galaxy samples

The Seyfert 2 galaxies sample is selected from the galaxy catalog of SDSS Data Release 4 (DR4). For our purpose, a redshift cut of $z < 0.3$ is used to ensure that the emission lines of interest, $H\alpha$, $H\beta$, $[O\ III]$ and $[N\ II]$, $[S\ II]$, fall in the spectra. We subtracted the stellar continuum to leave a clean emission line spectrum following the recipe described in Lu et al. (2006). In brief, we fit galaxy spectra with the templates derived by applying Ensemble Learning for Independent Component Analysis (EL-ICA) to the simple stellar population library (Bruzual & Charlot 2003). The templates were then broadened and shifted to match the stellar velocity dispersion of the galaxy. In this way, the stellar absorption lines are reasonably well subtracted to ensure reliable measurement of weak emission lines. Next, we fitted the emission line spectrum using gaussians (see next section) to derive emission line parameters. In practice, stellar subtraction and the emission line fitting are iterated because line parameters are used to create correct mask regions for emission lines during the stellar modeling. Only sources with $H\alpha$, $H\beta$, $[O\ III]$, $[N\ II]$ and $[S\ II]$ lines detected with $S/N > 5$ are considered for further study. Broad emission line objects are removed from the Seyfert 2 galaxies sample (described below). We adopt the criteria of Kewley et al. (2006) to classify the emission line galaxies as star forming galaxies, Seyfert galaxies, LINER, AGN/HII composites. For this study, we only stick to the classical Seyfert galaxies because only a very small fraction of Sy1s show a composite/LINER spectrum while there are large portion of such Sy2s. The final sample consists of 5544 sources.

Seyfert 1 galaxies¹ were drawn from quasar and galaxy catalogues of SDSS DR4 at redshift $z < 0.3$. For nucleus dominated sources where FeII multiplets and other broad emission lines are highly blended, we fit simultaneously the nuclear continuum, the FeII multiplets and emission lines (see Dong et al. 2008 for details). The nuclear continuum is

¹A small number of objects are in the luminosity range for quasars.

approximated by a broken power-law, with free indices for $H\alpha$ and $H\beta$ region respectively. Fe II emission, both broad and narrow, is modeled using the spectral data of the Fe II multiplets for I Zw 1 provided by Veron-Cetty et al. (2004). Emission lines are modeled as multiple gaussians. For those spectra with significant contribution of starlight as measured by the equivalent widths (EWs) of the Ca II K $\lambda 3934$ absorption line or high order Balmer lines or Na I $\lambda\lambda 5890, 5896$, a starlight model is also included using the 6 IC templates as described in the above. The decomposition of host-galaxy starlight, nuclear continuum and FeII emission were carried out following the procedure as described in detail in Zhou et al. (2006). We fit and subtracted the above model from the SDSS spectra, and then fit emission lines using multi-gaussian model (see next section).

Based on the fitted emission-line parameters, we construct the sample of Sy1s according to the criteria as follows. (1) Adding a broad gaussian component of $H\alpha$ to the model can improve the fit significantly with a chance probability less than 0.05 according to F-test; (2) The broad component is detected with $S/N \gtrsim 5$; (3) The peak of the broad component is at least twice the root-mean-square (rms) deviation in the regions surrounding $H\alpha$ (Dong et al., in prep). To guarantee the reliability of the measurements of the narrow lines of interest, we require that they have $S/N > 5$, the same as in the cases of Sy2s. Here the flux errors of narrow lines, especially $H\alpha$ and $H\beta$ narrow lines, have taken account for the uncertainty introduced by the emission-line modeling (Dong et al., in preparation). The final sample has 2768 Sy1s.

2.2. Emission Line Fitting

For Sy2s, after removing the starlight, we fit the emission-line spectra using the code described in detail in Dong et al. (2005). Briefly, every line is fitted with one or more Gaussians as is statistically justified (mostly with 1–2 Gaussians); the line parameters are achieved by minimizing χ^2 . The [O III] $\lambda\lambda 4959, 5007$ doublet lines are assumed to have the same profiles and redshifts; [N II] $\lambda\lambda 6548, 6583$ and [S II] $\lambda\lambda 6716, 6731$ doublet are constrained in the same way. Furthermore, the flux ratios of [O III] doublet and [N II] doublet are fixed to the theoretical values. Usually, $H\alpha$ line and [N II] doublet are highly blended and thus hard to isolate; in such cases, we fit them assuming they have the same profile as [S II] doublet, which is empirically justified (e.g., Filippenko & Sargent 1988; Ho et al. 1997; Zhou et al. 2006).

For Sy1s, once the nuclear continuum and the Fe II emission are subtracted, we perform a refined fit of the emission-line spectra. The narrow lines are modeled as for Sy2s. The broad lines are modeled with multi-gaussians, as many as is statistically justified. One concern is

the reliability of the decomposition of narrow and broad lines. We found that when the broad line is significantly broader than the narrow line and the narrow line is not weak, the flux of narrow line is trustworthy (Dong et al., in preparation). This is usually the case for narrow lines ($S/N > 5$) of Sy1s in this sample.

3. Results

3.1. A Comparison between Seyfert 1 and 2 galaxies

Dong et al.(2008) found that the distribution of broad-line Balmer decrement for blue AGNs is a gaussian in the logarithmic space, with a peak at 0.486 ($H\alpha/H\beta=3.1$) and an intrinsic standard deviation only ~ 0.03 . The reddening interpretation of large Balmer decrements is also supported by larger infrared to broad line ratio (Dong et al. 2005) and excess X-ray absorption in those objects (Wang et al. 2008). We estimate reddening to broad lines for objects with $H\alpha/H\beta$ significantly larger than the above value assuming a SMC extinction curve, by $E_{B-V}^b = 1.99 \times [\log(H\alpha/H\beta) - 0.486]$. Extinction to narrow lines is also estimated using the Balmer decrement and assuming an intrinsic narrow-line Balmer decrement of 3.1. Using the E_{B-V} and extinction curve, the intrinsic luminosities of $H\alpha$, $H\beta$ broad lines, as well as $H\alpha$, $H\beta$, $[O III]$ $[N II]$, $[S II]$ narrow lines can be calculated.

We plot the 5544 Sy2 and 2768 Sy1 sources on the BPT diagram in Figure 1. The intermediate broad line E_{B-V}^b group are not plotted for clarity. One can easily see that Sy1s and Sy2s apparently occupy different regions on BPT diagram. We defined a line (S12 line for short) such that Sy2s rarely appear on the left side:

$$\log([O III]/H\beta) = 3.53 \times \log([N II]/H\alpha) + 1.65 \quad (1)$$

Only 409 (7.3%) Sy2s lie on the left side of S12 line while 913 (33.0%) Sy1s on the left side. The overall trend is very clear that Sy1s lie to the left of Sy2s on the diagram. On average, $[N II]/H\alpha$ ratio is 0.11 dex higher in Sy2s than in Sy1s.

3.2. Seyfert 1 galaxies of different extinction

If we regard Sy2s as Seyfert galaxies with extremely high E_{B-V}^b in broad lines, the trend of different types of Seyfert galaxies should also be traced for Sy1s of different broad line extinction E_{B-V}^b . In the right panel of Fig 1, we split the source according to their E_{B-V}^b of broad emission lines. Only Sy1s in $E_{B-V}^b \in [0, 0.2]$ and $E_{B-V}^b \in [0.6, 1]$ are plotted for clarity. It is evident that as the E_{B-V}^b increases, the distribution moves to right. This is in

accordance with our hypothesis. One can see that a small fraction (23.8%) of objects in the $E_{B-V}^b \in [0.6, 1]$ group lie on the left side of S12 line while the fraction for the low extinction group is (43.3%).

3.3. On the narrow and broad line correlation

From the broad line sample, an empirical relationship between uncorrected [O III] luminosity and broad $H\alpha$ line luminosity can be obtained. The broad $H\alpha$ is corrected from the extinction to the broad line region as in last section.

$$\log(L_{[O\ III]}^{uncorrected}) = (0.977 \pm 0.007) \times \log(L_{H\alpha}^{intri}) + (0.238 \pm 0.294) \quad (2)$$

In Fig 2, we split the sample by their E_{B-V}^b and plot them on the [O III] vs $H\alpha$ diagram. The purple crosses are with low $E_{B-V}^b \in [0, 0.2]$ while green triangle symbols with high $E_{B-V}^b \in [0.6, 1]$. The average ratios (in logarithmic value) of luminosities of [O III] and $H\alpha$ for these two groups are -0.678 ± 0.278 and -1.012 ± 0.158 . Thus the [O III] luminosities of the low E_{B-V}^b group are on average two times (0.334 dex) larger than that of high E_{B-V}^b group at a given broad line luminosity. The mean values of the two groups are significantly different at a chance probability less than 10^{-10} according to the Student's t-test.

One concern is that this may be introduced by the biases that the measurement error in the E_{B-V}^b will lead to a shift in the relation for different E_{B-V}^b . However, Monte-Carlo simulation shows that it causes a deviation of only 0.06 dex for a typical $H\alpha$ luminosity, much smaller than the difference of 0.334 dex. Thus this must be real.

4. Discussion and conclusion

We find that Seyfert 1 galaxies have significantly smaller [N II]/ $H\alpha$ ratios than Seyfert 2 galaxies. A similar trend has also been observed in Sy1s with different BLR reddening: unreddened Seyfert 1 galaxies have smaller ratios than reddened ones. We also show that reddened Seyfert 1 galaxies have average lower uncorrected [O III] luminosity at a given nuclear luminosity represented by broad $H\alpha$ luminosity.

Before discussing the implication of these findings, we would like to rule out the possibility that they are introduced by systematic bias in our spectral modeling and sample selection. First, as a sanity check, we fit all the above-mentioned narrow lines assuming that they have the same profile; it does not change our results. Thus our findings are not caused by the emission-line modeling (different models for different lines). Second, stellar absorption

lines are properly subtracted in both Sy1s and Sy2s. We have visually inspected the high-order Balmer absorption lines to ensure they are well matched. Thus we are confident that the fluxes of narrow lines are not affected seriously by stellar absorption features. Third, we check Sy1s with either small difference in line width between broad lines and narrow lines, e.g., narrow line Sy1s, or with a relative low signal to noise ratio, where the decomposition of narrow and broad components is most difficult. We find that their location on BPT diagram is indistinguishable from other Sy1s. Therefore, the line-profile decomposition should not affect our results. Last, but not the least, we check the influence of our sample selection by raising the criterion for the S/N of narrow line to be 7. We find that the fraction of objects lying on the left side of S12 line is 9% for Sy2s, 26.4% for Sy1s in the $E_{B-V}^b \in [0.6, 1]$ group and 44.6% for Sy1s in the $E_{B-V}^b \in [0, 0.2]$ group. These values are almost the same as those presented in §3.

Let's consider the fact that there are substantial Sy1s with very low $[\text{N II}]/\text{H}\alpha$ first. Low $[\text{N II}]/\text{H}\alpha$ can be produced with very metal poor gas (Groves et al. 2006), or presence of gas with a density above the $[\text{N II}]$ critical density with high ionization. We argue that metal-poor gas hypothesis is unlikely. Groves et al. showed that gas metallicity is correlated with the mass of galaxy bulge, which is in turn correlated with central black hole mass. However, we find that Sy1s on the left of S12 line have a similar black hole mass distribution as the whole sample. Furthermore, if the metal-poor gas hypothesis is right, then the fact that this group almost does not have type 2 counterparts is directly in contrast to the well-supported unification scheme.

The different distribution of Sy1s and Sy2s on BPT diagram does not suggest the failure of AGN unification because reddened Sy1s show a distribution in between. Rather it can be interpreted as partial obscuration to the NLR in Sy2s. It is well established that the NLR is stratified with high density and high ionization gas at close to the continuum source whereas low density and low ionization gas is in outer part of NLR (Nagao et al. 2003, Riffel et al. 2006). At high densities, lines with low critical densities, such as $[\text{N II}]$, $[\text{S II}]$, are suppressed by collisional de-excitation process, while lines with high critical densities and recombination lines, are unaffected. Considering $[\text{O III}]$ is the dominant narrow line in Sy1s, we hypothesis that even in the inner NLR, the gas density does not exceed the critical density of $[\text{O III}]$, i.e., $[\text{O III}]$, $\text{H}\alpha$ and $\text{H}\beta$ trace each other in the inner NLR. Once the inner NLR is obscured by opaque dusty material in Sy2s, one would expect that the $\text{H}\alpha$ emitting region to be shielded while $[\text{N II}]$ emitting region being affected to a less degree or not at all, thus the $[\text{N II}]/\text{H}\alpha$ ratio will be shifted to a larger value while $[\text{O III}]/\text{H}\beta$ remains the same. The uncorrected $[\text{O III}]$ luminosity of reddened Sy1s are underluminous in comparison with unreddened one

is consistent with the partial obscuration interpretation ².

The obscuring material can be the extended part of the torus or a dusty lane in the host galaxy. The inner edge of dusty torus is known to be order of parsecs from the central engine (Rhee et al. 2006), but the extent and height of the torus are not well constrained. Schmitt et al. (2003) showed that all Sy1s have a resolved bright [O III] emission knot at the nucleus on the scales typically tens parsecs, and half [O III] emission radius is typically tens parsecs. Thus, combined with their result, our findings here suggest that, at least in a large fraction ($\gtrsim 30$ per cent) of AGNs if not all, the obscuring material (likely being the torus) must extend to several tens of parsecs.

We thank Guinevere Kauffmann and Xue-Guang Zhang, as well as the anonymous referee for critical comments. We also thank Ting Xiao and Shaohua Zhang for useful discussion. This work is supported by Chinese NSF grants NSF-10533050 and NSF-10573015, the Knowledge Innovation Program (Grant No. KJCX2-YW-T05). Funding for the Sloan Digital Sky Survey (SDSS) has been provided by the Alfred P. Sloan Foundation, the Participating Institutions, the National Aeronautics and Space Administration, the National Science Foundation, the U.S. Department of Energy, the Japanese Monbukagakusho, and the Max Planck Society. The SDSS is managed by the Astrophysical Research Consortium (ARC) for the Participating Institutions. The SDSS Web site is <http://www.sdss.org/>.

REFERENCES

- Antonucci, R. 1993, ARA&A,31, 473
- Antonucci, R. & Miller, 1985, ApJ,297, 621
- Baldwin, J. A., Phillips, M. M., & Terlevich, R., 1981, PASP, 93, 5
- Barthel, P. D. 1994, The Physics of Active Galaxies, 54, 175
- Barthel, Peter D., 1989, ApJ, 336, 606
- Best, P., Röttgering, H., & Longair, M. 1999, Activity in Galaxies and Related Phenomena, 194, 241

²If the obscuring material is opaque and covers only the inner part of NLR, narrow line flux will be smaller. Meanwhile, due to its small size, the BLR is entirely covered by dust and the broad lines can be efficiently corrected from Balmer decrement.

- Bruzual, G.; Charlot, S., 2003 ,MNRAS, 344, 1000
- Dong, X.-B., Zhou, H.-Y., Wang, T.-G., Wang, J.-X., Li, C., & Zhou, Y.-Y. 2005, ApJ, 620, 629
- Dong, X. B; Wang, T. G; Wang, J. G; Yuan, W. M; Zhou, H. Y; Dai, H. F; Zhang, K 2008, MNRAS, 383, 581
- Filippenko, A. V., & Sargent, W. L. W. 1988, ApJ, 324, 134
- Greenhill et al, 2003, ApJ, 590,162
- Groves, Brent A.; Heckman, Timothy M.; Kauffmann, Guinevere, 2006, MNRAS, 371, 1559
- Haas, M., Siebenmorgen, R., Schulz, B., Krügel, E., & Chini, R. 2005, A&A, 442, L39
- Ho, L. C., Filippenko, A. V., Sargent, W. L. W., & Peng, C. Y. 1997, ApJS, 112, 391
- Jackson, N. & Browne, I. W. A. 1990, Nature, 343, 43
- Jaffe et al, 2004 , ApJ, 615, 55
- Kewley, L. J., Groves, B., Kauffmann, G., & Heckman, T., 2006, MNRAS, 372, 961
- Klöckner, H.-R., Baan, W. A., & Garrett, M. A. 2003, Nature, 421, 821
- Lu, H., Zhou, H., Wang, J., Wang, T., Dong, X., Zhuang, Z., & Li, C. 2006, AJ, 131, 790
- Meisenheimer, K.; Haas, M.; Mller, S. A. H.; Chini, R.; Klaas, U.; Lemke, D., 2001, A&A, 372, 719
- Miller, J. S.; Goodrich, R. W., 1990, ApJ, 355, 456
- Murayama, Takashi; Taniguchi, Yoshiaki, 1998, ApJ, 503L, 115
- Nagao, Tohru; Murayama, Takashi; Shioya, Yasuhiro; Taniguchi, Yoshiaki, 2003, AJ, 126, 1167
- Ogle, Patrick; Whysong, David; Antonucci, Robert, 2006, ApJ, 647, 161
- Rhee, Joseph H.; Larkin, James E., 2006, ApJ, 640, 625
- Riffel, R.; Rodrguez-Ardila, A.; Pastoriza, M. G., 2006, A&A, 457, 61
- Robinson, A. et al. 1994, A&A, 291, 351

Schmitt, H. R. 1998 ,ApJ, 506, 647

Schmitt, H. R.; Donley, J. L.; Antonucci, R. R. J.; Hutchings, J. B.; Kinney, A. L.; Pringle, J. E., 2003, ApJ, 597, 768

Tristram, K. R. W. et al. 2007, A&A, 474, 837

Veilleux, S., & Sylvain, 1991, ApJ, 369, 331

Véron-Cetty, M.-P., Joly, M., & Véron, P. 2004, A&A, 417, 515

ang T. G. et al , AJ, submitted

York, D. G. et al. 2000, AJ, 120, 1579

Zhou, H., Wang, T., Yuan, W., Lu, H., Dong, X., Wang, J., & Lu, Y. 2006, ApJS, 166, 128

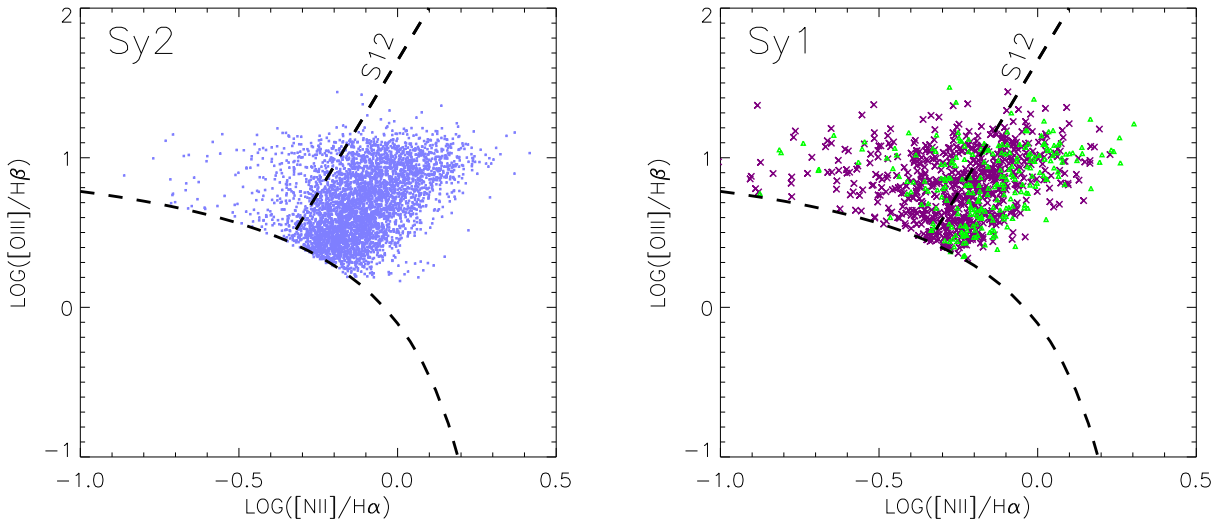


Fig. 1.— BPT diagram for Seyfert 1 (right panel) and Seyfert 2 (left panel) galaxies. The lower curve is the empirical line separating AGN from star-forming galaxies (Kewley et al 2006). The straight line is the S12 line described in the text. Most Seyfert 2 galaxies locate on the right side of the line. In the right panel, purple crosses represent objects with $E_{B-V}^b < 0.2$ and green triangles those with $E_{B-V}^b \in [0.6, 1]$ while the intermediate E_{B-V}^b group are not plotted for clarity.

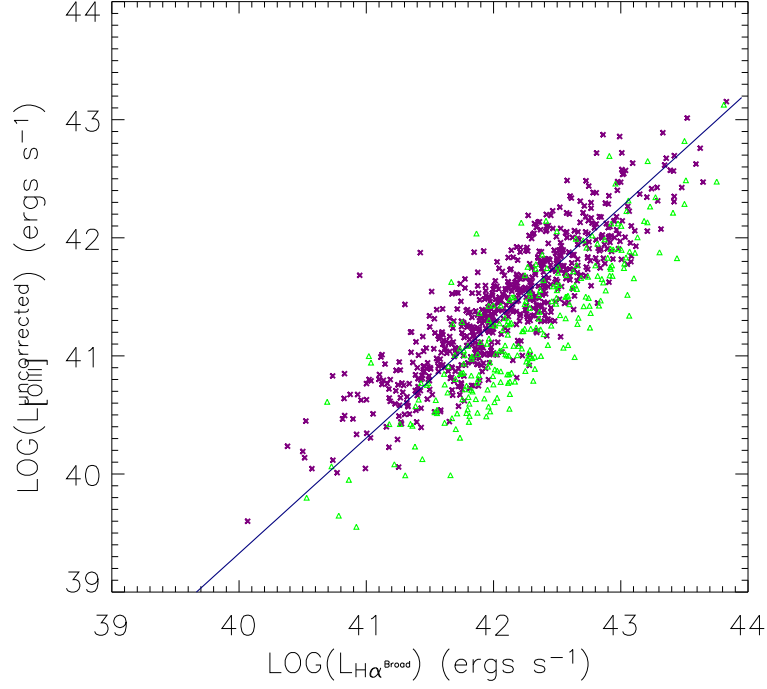


Fig. 2.— The uncorrected luminosity of [O III] versus extinction corrected luminosity of broad H α for Seyfert 1 galaxies. The purple crosses are AGNs with $E_{B-V}^b < 0.2$ and green triangles with $E_{B-V}^b \in [0.6, 1]$. The blue line shows the best linear fit to the whole sample. The intermediate E_{B-V}^b group is not plotted for clarity.